Los Alamos National Laboratory is operated by the University of California for the United States Department of Energy under contract W-7405-ENG-36

LA-UR--87-3053

DE88 000526

TITLE PION-INDUCED MESON PRODUCTION IN NUCLEI -- (π,η) AND THE (π^+,K^+) REACTIONS

AUTHOR(S) J. C. Peng

SUBMITTED TO Proceedings of International Symposium on Medium Energy Physics, Beijing, China, June 23-27, 1987

DISCLAIMER

Los Alamos Los Alamos National Laboratory
Los Alamos, New Mexico 87545

PION-INDUCED MESON PRODUCTION IN NUCLEI – THE (π,η) AND THE (π^+,K^+) REACTIONS

J. C. Peng
Los Alamos National Laboratory
Los Alamos, New Mexico 87545
USA

ABSTRACT

The subject of meson productions in nuclei, a new direction in pion-nucleus physics, is discussed. Recent experimental results at LAMPF and AGS on the (π,η) and (π^+,K^+) reactions in nuclei are presented.

I. INTRODUCTION

The subject of pion-nucleus interaction has been extensively studied during the last decade at several meson factories. Some examples of such studies, namely, the pion-induced single and double charge-exchange reactions and pion absorption in nuclei, have been discussed in this symposium. In order to obtain a global picture of meson-nucleus interaction, it is very desirable to investigate not only the interaction between pion and nuclei, but also the interaction between other heavier mesons and nuclei. In this talk, I will report on the (π,η) and (π,K) experiments recently performed at LAMPF and at AGS. These experiments represent some of the first efforts to study pion-induced heavy mesons productions in nuclei.

The subject of pion-induced heavy meson production in nuclei is just beginning to be explored. There exist very few experimental data on this subject. This situation is mostly due to the fact that relatively high energy pion beams are required for such experiments. In Fig. 1 we show the thresholds for producing various mesons on nucleon with pion beam. The energies of the pion beam at the existing meson factories such as SIN and TRIUMF are not sufficiently high to produce these heavy mesons. Fortunately, as shown in Fig. 1, the threshold for coherent meson productions on nuclear targets are significantly lowered. In this talk, I will focus on the production of two of the lightest mesons, namely the eta meson and the kaon.

II. (π,η) REACTION IN NUCLEI

Before discussing the (π,η) reaction, it is useful to review briefly some properties of the η meson. In a certain sense, the eta meson can be considered as a heavy Λ^0 meson. It is instructive to compare the η meson with the π^0 meson and the η' meson. Some properties of the π^0, η, and η' mesons are listed in Table I.[1] These three mesons, as

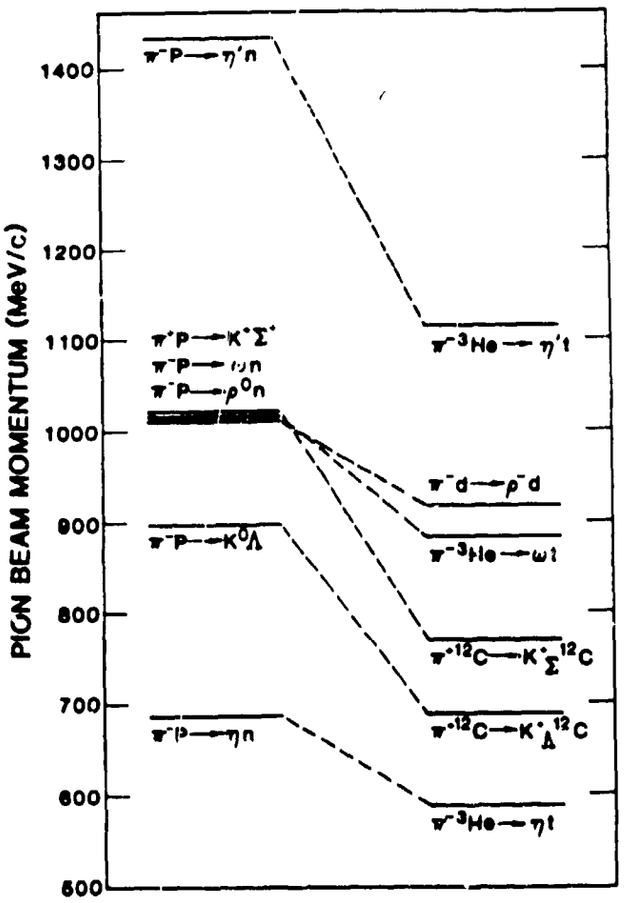

Fig. 1. Thresholds for pion-induced meson productions on nucleon and on nuclear targets.

members of the pseudoscalar meson nonet, have identical spin, parity and C-parity. A major difference between the η, η' mesons and the π^0 meson is in their isospin. The η, η' mesons, being isoscalar particles, can have $s\bar{s}$ and $c\bar{c}$, in addition to the $u\bar{u}$ and $d\bar{d}$, as their quark contents. Table I lists the pure SU(3) quark wave functions for these mesons. The relatively large mass of η, η' reflects the strange quark $s\bar{s}$ components in them. Similar to the π^0 meson, which decays predominantly into two photons, the η meson also decays into two photons with a large fraction. Indeed, detections of the π^0, η and η' mesons are usually made through the measurement of the photon pair.

In addition to using pion beam to produce η meson, one could also use medium energy proton, kaon, and photon beams. The (π, η) reaction has the advantage that the cross section is rather large. Figure 2 shows the integrated cross sections[3] of the $\pi^- p \to \eta n$ reaction as a function of beam energy. The cross section peaks at energy very close to the threshold. Fortunately, the maximum pion beam energy at Los Alamos

TABLE I. Properties of π°, η and η' mesons

	π°	η	η'
J^{PC}	0^{-+}	0^{-+}	0^{-+}
(I, I_3)	(1,0)	(0,0)	(0,0)
Quark w.f.	$(u\bar{u} - d\bar{d})/\sqrt{2}$	$(u\bar{u} + d\bar{d} - 2s\bar{s})/\sqrt{6}$	$(u\bar{u} + d\bar{d} + s\bar{s})/\sqrt{3}$
Mass	134.9 MeV	548.8 MeV	957.6 MeV
Mean life	$0.83 \times 10^{-16} sec$	$0.75 \times 10^{-18} sec$	$0.28 \times 10^{-20} sec$
2γ decay fraction	98.8%	39%	2%

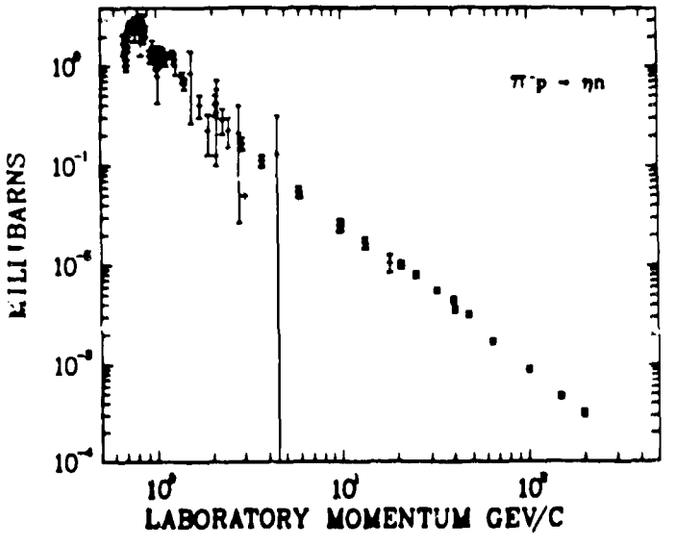

Fig. 2. Integrated cross section of the $\pi^- p \to \eta n$ reaction.

is slightly above the $\pi^- p \to \eta n$ threshold. Furthermore, the threshold is significantly lowered for (π, η) reaction on nuclear targets and intense pion beams are available at these energies.

At the time we proposed to measure the (π, η) reaction at LAMPF, there existed, not surprisingly, very few experimental data[3-6] on the (π, η) reaction on nuclear targets. These data were obtained with very high energy pion beam and only inclusive η spectra were measured due to relatively poor energy resolution. Our LAMPF experiments[7] ex-

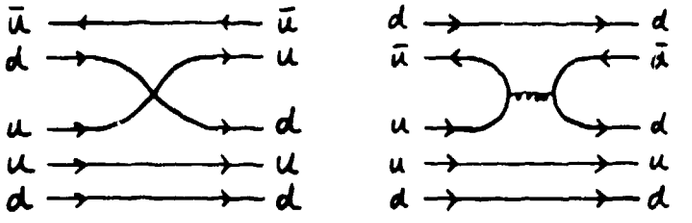

Fig. 3. Quark diagrams for the $\pi^- p \to \pi^0 n$ and $\pi^- p \to \eta n$ reactions.

plore the (π, η) reaction at energies near or even below the free threshold. Furthermore, we proposed not only to measure the inclusive η spectra but also to look for any discrete states excited in the (π, η) reaction. Clearly, adequate energy resolution is required for identifying discrete states.

We will now present some of the physics issues concerning the (π, η) reaction on nuclear targets.

a. $(\pi^{\pm}, \eta)$ as a charge-exchange reaction

The $(\pi^{\pm}, \eta)$ can be regarded as exotic charge-exchange reactions. It is interesting to compare the $(\pi^{\pm}, \eta)$ with the more conventional and extensively studied $(\pi^{\pm}, \pi^0)$ charge-exchange reaction. Figure 3 shows the two quark diagrams contributing to the (π^-, π^0) and (π^-, η) reactions. The first diagram involves quark exchange and leads to the $u\bar{u}$ component of the π^0, η wave functions. The second diagram shows that annihilation and creation of $q\bar{q}$ pairs are responsible for producing the $d\bar{d}$ component. It is important to note that there is no quark diagram which can lead to the $s\bar{s}$ component in η.

Since the $\pi^{\pm}, \pi^0$ belong to the same isospin multiplet, the $(\pi^{\pm}, \pi^0)$ charge-exchange reactions are closely related to $\pi^{\pm}$ elastic scattering. In fact, the $(\pi^{\pm}, \pi^0)$ reactions reflect the isospin dependence of the π-nucleus interaction. The $(\pi^{\pm}, \eta)$ reactions, on the other hand, involves a pair of particles having different isospins. Therefore, the $(\pi^{\pm}, \eta)$ reactions reveal the reactive content of the π-nucleus interaction.

It should also be mentioned that in the (π, η) reaction the momentum transfer, $\sim$250 MeV/c at 0°, is large compared with the (π, π^0) reaction. While $(\pi^{\pm}, \pi^0)$ reactions are suitable for exciting low spin states such as Isobaric Analog States (IAS),[8] the $(\pi^{\pm}, \eta)$ reactions are expected to excite more favorably high spin states.

b. N* resonances

While the πN system can couple to both Δ^* and N* resonances, the ηN system can only couple to N* resonances. Table II shows that the N*(1440)P_{11}, N*(1535)S_{11} and N*(1710)P_{11} resonances have large branching ratios to the ηN channel. The N*(1535)S_{11}

TABLE II. Coupling between N^* and ηN

Resonance	J^P	L_{2I2J}	ηN Branching
$N^*(1440)$	$\frac{1}{2}^+$	P_{11}	$8-18\%$
$N^*(1535)$	$\frac{1}{2}^-$	S_{11}	$45-55\%$
$N^*(1710)$	$\frac{1}{2}^+$	P_{11}	$\sim 25\%$

resonance is known to play a dominant role[9] in the $\pi^- p \rightarrow \eta N$ reaction at threshold energies. The coupling between the N*(1440) Roper resonance to the ηN channel is less well established. Since the N*(1440) Roper resonance lies below the ηN threshold, one expects that subthreshold η production on nuclear targets could be sensitive to the Roper resonance. A similar situation occurs in the $K^- N$ system, where subthreshold Y* resonances greatly influence the $K^- N$ interaction at thresbold energies.

c. η-nucleus interaction

Since the η meson is too short-lived to be used as a beam, there exists very little information on η-nucleon and η-nucleus interactions. Production of η mesons inside a nucleus allows us to deduce these interactions.

In the SU(3) model, the ηN coupling constant $G_{\eta NN}$ is related to the πN coupling constant $G_{\pi NN}$ by the relation[10]

$$G_{\eta NN} = G_{\pi NN}(3-4\alpha)/\sqrt{3} \ .$$

where $\alpha = D/(D+F)$, and D,F are the strengths of coupling in SU(3). The hyperon decay experiments give $0.60 < \alpha < 0.66$, therefore, SU(3) predicts $G^2_{\eta NN}/G^2_{\pi NN}$ to be between 0.043 and 0.12. This shows that the ηN interaction is expected to be much weaker than the πN interaction. One could understand qualitatively this situation by realizing that the $s\bar{s}$ component in η does not contribute to the ηN interaction.

The $G_{\eta NN}$ can also be deduced from the description of NN force by One-Boson-Exchange Model. It is generally believed that the effect of η-meson exchange is small and the deduced value[11] of $G^2_{\eta NN}/G^2_{\pi NN}$ is 0.29 in the most recent tabulation.

Another quantity relevant to the ηN interaction at low energy is the scattering length. In a K-matrix analysis of the $\pi^- p \rightarrow \eta N$ reaction, Tuan[12] deduced the ηN scattering length to be $0.83 + i0.05 fm$. More recently, Bhalerao and Liu[13] use isobar model to analyse a more complete set of $\pi^- p \rightarrow \eta N$ data and obtain a value of

TABLE III. Summary of η-meson production measurements at LAMPF

Date	Reactions	Apparatus
Sept. '84	$p(\pi^-,\eta)n$ $^{12}C(\pi^-,\eta)$	neutron detectors BGO ($\eta \rightarrow 2\gamma$ detection)
June '85	$^3He(\pi^-,t)\eta$	LAS spectrometer (triton detection)
Oct. '85	$p(\pi^-,\eta)n$ $^3He(\pi^-,\eta)t$ $^7Li(\pi^+,\eta)^7$ Be (π^+,η) inclusive	π^0-spectrometer (Pb glass) ($\eta \rightarrow 2\gamma$ detection)
Oct. '86	$d(\pi^\pm,\eta)$ $(\pi^\pm,\eta)$ inclusive	η-spectrometer (NaI + BGO) ($\eta \rightarrow 2\gamma$ detection)

$0.28 + i0.19 fm$. Although these two analyses give different magnitude of the scattering length, they both predict that the real part of the ηN interaction is attractive. This led to the prediction[14,15] that η-nucleus bound states could exist. Since an η in nucleus can undergo strong interactions such as $\eta N \rightarrow \pi N$, $\eta N \rightarrow \pi\pi N$, and $\eta N \rightarrow \pi\pi\pi N$, it is not clear[14] that the widths of η-nucleus states are sufficiently narrow to be observed experimentally. As will be shown later, the total ηN cross sections can be deduced from the mass dependence of the (π,η) inclusive cross section.

III. (π,η) EXPERIMENTS AT LAMPF

During the last two years, there have been several (π,η) experiments carried out at LAMPF. Table III lists these experiments. A number of different apparatus, including neutron detectors, charged particle spectrometer and photon spectrometers, have been used in these experiments. We will now discuss the set-ups and some preliminary result from these experiments.

a. $^3He(\pi^-,t)\eta$ reaction[16]

The ^3He target is of interest since the $^3He(\pi^-,\eta)t$ reaction can be identified by detecting either the η mesons or the recoiled tritons. Furthermore, the structure of ^3He and triton are relatively simple so that theoretical analysis of this reaction is less subjected to uncertainties in nuclear structure. Finally, the $^3He(\pi^-,\pi^0)t$ charge-exchange reaction

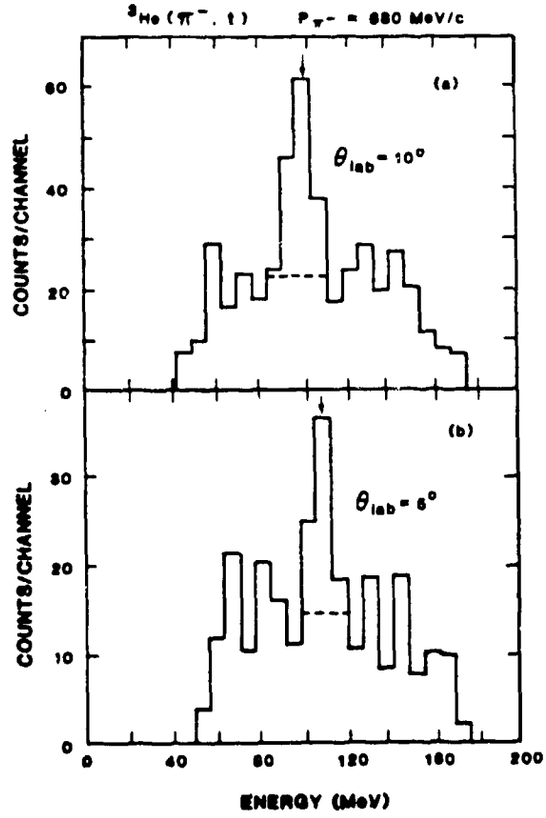

Fig 4. Triton energy spectra measured in the $^3He(\pi^-,t)$ reaction. The arrows indicate the expected location of the $^3He(\pi^-,t)\eta$ reaction. The dashed lines indicate the background estimate.

has been studied in great detail both theoretically[17] and experimentally.[18] This allows us to compare the $^3He(\pi^-,\eta)t$ reaction with the $^3He(\pi^-,\pi^0)t$ reaction.

The experiment was performed with 680 MeV/c π^- beam incident on a cryogenic ^3He target.[19] The outgoing tritons were detected with a Large Acceptance Spectrometer (LAS).[20] The TOF and momentum measurements provided unambiguous triton identification. Figure 4 shows the triton spectra at $\theta_{lab} = 5°$ and 10°. A peak is clearly observed at an energy expected for the binary reaction $^3He(\pi^-,t)\eta$. In addition to this peak, one observes a continuum background which is believed to come from the $^3He(\pi^-,t)\pi\pi$ and $^3He(\pi^-,t)\pi\pi\pi$ multi-pion production reactions.

Figure 5 shows the measured cross sections for the $^3He(\pi^-,\eta)t$ reaction at backward angles. It is remarkable that the observed cross sections are rather sizable despite the large momentum transfer ($\sim 800 MeV/c$) and the fact that the beam momentum is already below the $P(\pi^-,\eta)n$ threshold (686 MeV/c). The $p+d \rightarrow {}^3He+\eta$ cross sections[21] are more than three orders of magnitude lower than those of the $\pi^- + {}^3He \rightarrow \eta + t$

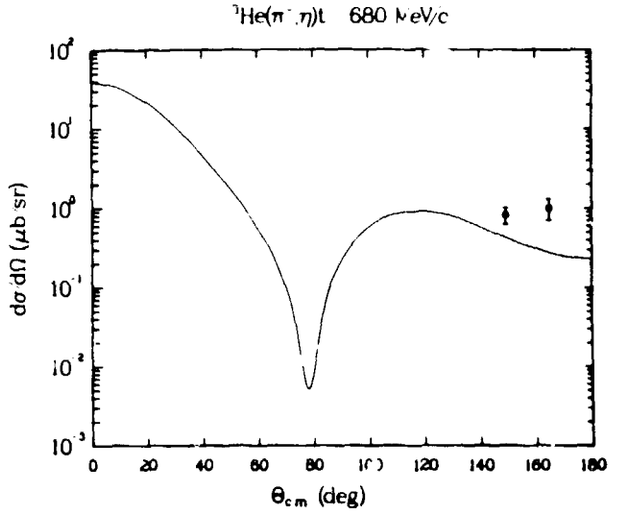

Fig. 5. Cross sections measured in the $^3He(\pi^-,\eta)t$ reaction. The solid curve is result of DWIA calculation.

reaction. The back-angle ($\theta_{c.m.} \simeq 140°$) cross section for the $^3He(\pi^-,\pi^0)t$ reaction measured[18] at 406 MeV/c is about a factor of 10 larger than the $^3He(\pi^-,\eta)t$ cross sections. One would expect this factor to be significantly larger, since the $p(\pi^-,\pi^0)n$ cross section at 406 MeV/c is $\sim 20mb$ while the Fermi-averaged $p(\pi^-,\eta)n$ cross section at 680 MeV/c is $\sim 1mb$. Furthermore, the momentum mismatch in the $^3He(\pi^-,\eta)t$ reaction is more severe than in the $^3He(\pi^-,\pi^0)t$ reaction. Therefore, it appears that the observed $^3He(\pi,\eta)t$ cross sections are larger than expected from simple considerations.

Theoretical studies on the $^3He(\pi,\eta)t$ reaction have been carried out using Distorted Wave Impulse Approximation (DWIA). The $\pi N \rightarrow \eta N$ and $\eta N \rightarrow \eta N$ amplitudes used in the DWIA calculations were obtained from an off-shell model (OSM)[15] in which reactions proceed by the formation of N* isobars. The parameters in this model were determined from the πN phase shift alone and the existing $\pi^- p \rightarrow \eta N$ cross sections near threshold energies were well described by this model. The nuclear form factors of ^3He and triton were taken from electron scattering experiments. Results of the DWIA calculation is shown as the solid curve in Fig. 5. The DWIA predicts a diffractive shape for the angular distribution which has a minimum near $\theta \simeq 80°$. The observed cross sections at the backward angles are greater than the prediction by a factor of 2-4.

To make a more detailed comparison between the data and theory, it is clearly desirable to measure the $^3He(\pi,\eta)t$ cross sections at forward angles. This requires detecting η mesons directly and is the next subject we will discuss.

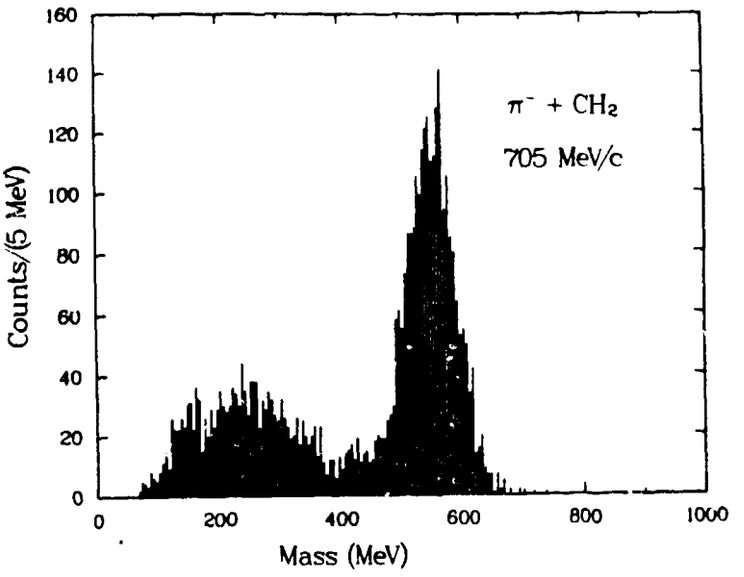

Fig. 6. Invariant mass spectrum for the 2γ detected in the $\pi^- + p$ reaction at 705 MeV/c.

b. Subthreshold production of the $^3He(\pi,\eta)t$ reaction

The LAMPF π^0 spectrometer,[22] designed to measure π^0 mesons with reasonably good energy resolution and solid angle acceptance, was used in this experiment to detect the $\eta \rightarrow 2\gamma$ decays. In order to understand the characteristics of this spectrometer, we first measured the $\pi^- p \rightarrow \eta n$ reaction. Figure 6 shows the histogram of the invariant mass calculated with the expression $m = 2(E_1 E_2)^{1/2} sin(\psi/2)$, where E_1, E_2 are the measure energies of the two photons and ψ is the opening angle between them. The η peak shows up very clearly in the invariant mass plot. The η energy resolution is $\sim 10MeV$, which is mainly due to the beam ($\Delta E = 7MeV$) and the target thickness.

The invariant mass plot for the $\pi^- + {}^3He$ reaction at 680 MeV/c is shown in Fig. 7. Once again, the η events are well identified in the mass plot. Figure 8 shows the preliminary excitation energy spectra of the $^3He(\pi^-,\eta)$ reaction measured at three pion beam momenta. At 680 MeV, which is near the free $p(\pi^-,\eta)n$ threshold, the $^3He(\pi,\eta)t$ reaction appears as a shoulder of the quasi-free $^3He(\pi,\eta)$ reaction. As the beam momentum is lowered to 620 MeV/c, the separation between the ground state transition and the quasi-free continuum improves greatly. At 590 MeV/c pion momentum, which is just above the absolute threshold of the $^3He(\pi,\eta)t$ reaction and below the threshold of any other $^3He(\pi,\eta)$ channels, the $^3He(\pi,\eta)t$ reaction is unambiguously detected. It is intriguing that the subthreshold (π,η) reaction has such an appreciable cross sections. Several efforts[23,24] to calculate the (π,η) cross section on nuclei are underway. In particular, a DWIA calculation[24] by Liu describes the shape of the $^3He(\pi,\eta)t$ angular distribution rather well, but underestimates the magnitude by a factor of ~ 2.

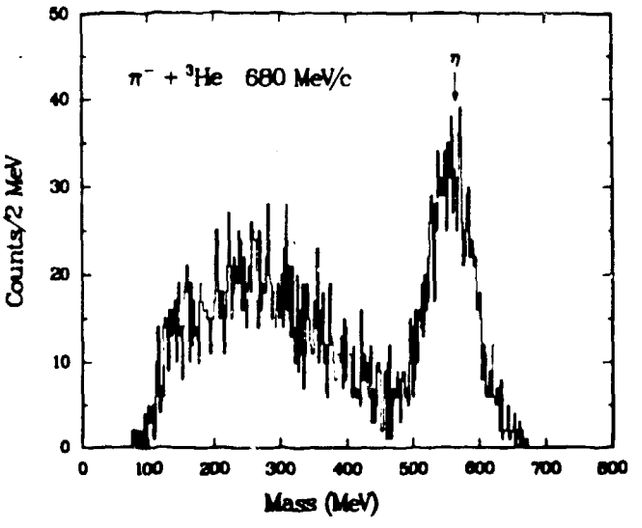

Fig. 7. Invariant mass spectra for the 2γ detected in the $\pi^- + {}^3He$ reaction at 680 MeV/c.

c. (π^+, η) inclusive cross sections

Figure 9 shows the energy-integrated (π^+, η) inclusive cross sections on a number of nuclei measured at three pion momenta. In an attempt to understand the observed mass dependence of the (π^+, η) inclusive cross sections, we use a version of the Glauber theory developed by Kolbig and Margolis.[25] In this model, the inclusive cross section is proportional to the effective nucleon number N_{eff}. The ingredients for calculating N_{eff} are the nucleon density distribution, the hadron-nucleon total cross sections for the incident and the outgoing particles. The only unknown input in this calculation is the total cross section for ηN. The various curves on Fig. 9 correspond to calculations using values of $\sigma(\eta N)$. A good description of the mass dependence at all beam momenta is obtained with $\sigma(\eta N) = 15mb$. The extracted ηN total cross section is rather small compared to the πN total cross section of 34 mb at this energy. This is in qualitative agreement with the theoretical expectation[10] that ηN interaction is weaker than the πN interaction.

It is interesting to note that in the additive quark model,[26] the ηN total cross section is related to the πN and KN total cross section as

$$\sigma\eta_N = \frac{1}{3}(\sigma_{K^+p} + \sigma_{K^-p} + \sigma_{K^+n} + \sigma_{K^-n}) - \frac{1}{6}(\sigma_{\pi^+p} + \sigma_{\pi^-p}) \ .$$

Figure 10 shows that the prediction of the additive quark model is in rather good agreement with the data, most of which were obtained at much higher energies. For the sake of comparison, $\sigma_{\pi N}$ is also shown in Fig. 10. The ηN total cross sections are clearly lower than the πN total cross sections over a wide energy range.

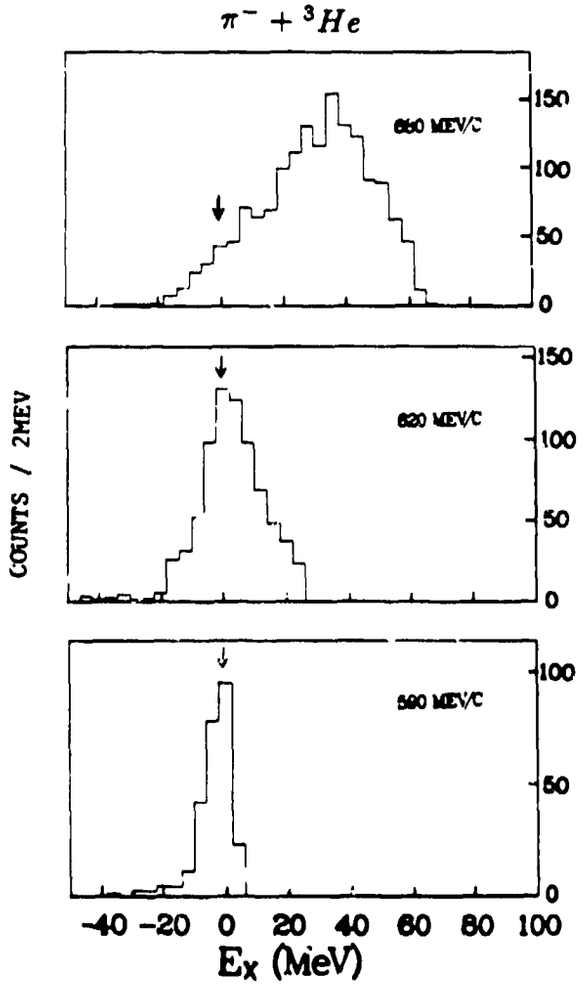

Fig. 8. η energy spectra measured in the ${}^3He(\pi^-,\eta)$ reaction at three π^- momenta. The arrows indicate the location of the ${}^3He(\pi^-,\eta)t$ transition.

Very recently, we have made more measurements on the (π,η) reaction using the eta-spectrometer. The eta-spectrometer is very similar to the LAMPF π^0-spectrometer. However, BGO and NaI crystals, rather than lead glass, were used for the converters and shower detectors. The data obtained with the eta-spectrometer are currently being analysed.

In summary, the $(\pi^\pm,\eta)$ reactions have been measured on several nuclei near and below the free threshold. The energy resolutions achieved in these experiments were sufficiently good that a discrete nuclear state is observed in the ${}^3He(\pi^-,\eta)t$ reaction. Improved beam quality ($\Delta E \sim 1$ MeV) would be required for observing discrete states in heavy nuclei. From the mass dependence of the (π^+,η) inclusive cross sections, we have extracted the ηN total cross section at threshold energies. The result, $\sigma(\eta N) < \sigma(\pi N)$, is consistent with the prediction of additive quark model. The (γ,η) and (p,η) reactions on

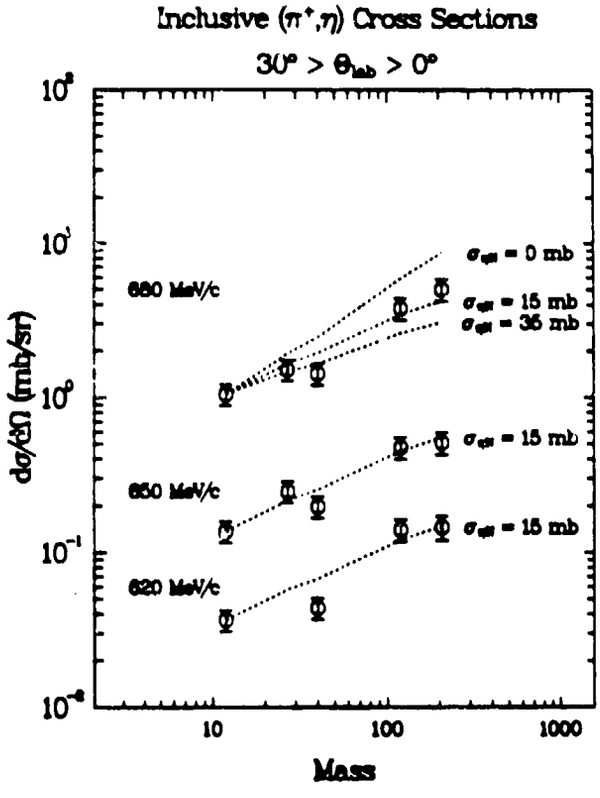

Fig. 9. Inclusive (π^+, η) cross sections on several target nuclei. The dashed curves correspond to Glauber calculations using various ηN total cross sections.

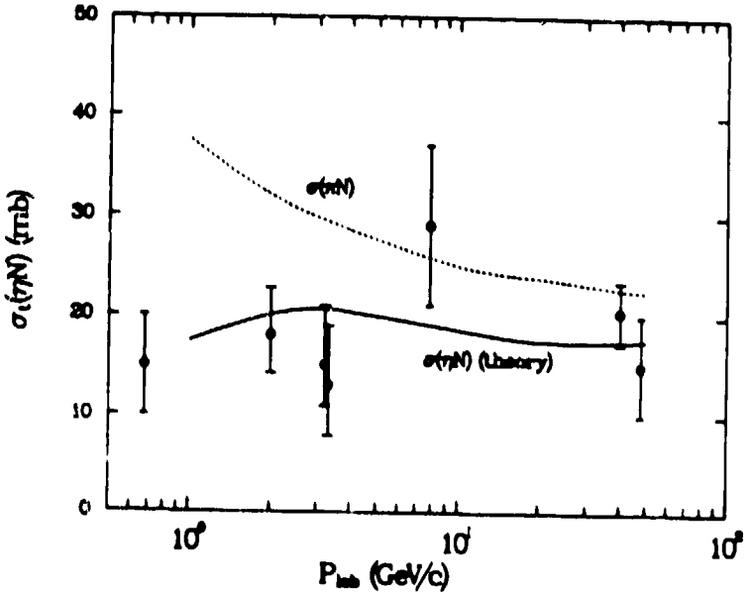

Fig. 10. ηN total cross sections as a function of P_{lab}. The solid curve is a prediction of ηN total cross section based on additive quark model. The dashed curve shows the πN total cross section.

nuclear targets are also of interest and several experimental proposals to measure these reactions already exist. It would also be most interesting to study the production of other massive mesons ($\rho, \omega, \sigma, \eta'$, etc.) in nuclei with more energetic pion beams.

IV. (π^+, K^+) EXPERIMENTS AT AGS

The major physics motivation for measuring the (π^+, K^+) reaction in nuclei is to study hypernuclei. For more than a decade, the (K^-, π) reaction has been the most important tool[27] to produce hypernuclei. In this strangeness-exchange reaction, the strange quark is brought in by the kaon beam and subsequently transferred to the target nucleus to form a hypernucleus. The meager kaon flux available in existing accelerators has limited the usefulness of the (K^-, π) reaction. In particular, high-spin hypernuclear states, which are expected to be weakly populated in the (K^-, π) reaction, have never been identified.

It is clear that hypernuclei can be produced by reactions other than the (K^-, π). These reactions usually fall into the category of associated productions, in which a pair of s and $\bar{s}$ quarks are produced. Examples of such associated productions are the (π^+, K^+), (p, K^+), (γ, K^+) and the $(\bar{p}, \bar{\Lambda})$ reactions. In particular, Dover, Ludeking and Walker[28] investigated the theoretical aspects of the (π^+, K^+) reaction as a spectroscopic tool for hypernuclear physics. The first (π^+, K^+) experiments, proposed by Thiessen,[29] was performed at the AGS accelerator in 1983. The feasibility of the (π^+, K^+) reaction for hypernuclear spectroscopy was clearly demonstrated in this first (π^+, K^+) experiment, in which the $^{12}C(\pi^+, K^+)$ reactions leading to the $^{12}_{\Lambda}C(g.s.)$ and $^{12}_{\Lambda}C(2^+)$ states were unambiguously identified.[30]

The sizable cross section observed in the $^{12}C(\pi^+, K^+)\,^{12}_{\Lambda}C(g.s.)$ transition suggested that deeply bound Λ-hypernuclear states (including the ground state) can be favorable studied by the (π^+, K^+) reaction. A systematic investigation of such deeply bound hypernuclear states is of great interest for two reasons. First, the existing information on the Λ-hypernuclear binding energy, deduced from emulsion data, was restricted to only light nuclei ($A < 16$).[31] Experimental data on the binding energies of medium and heavy hypernuclei are crucial for determining the Λ-binding energy in nuclear matter. Second, it was suggested[32] that the up and down quarks constituents of a Λ-particle deeply bound inside the nuclei may experience the Pauli repulsion generated by the surrounding nucleons. This conjectured partial-deconfinement of Λ-particle inside nuclei could lead to unusual behavior in the binding energies of such states. The potential of the (π^+, K^+) reaction for studying heavy hypernuclei prompted two new experimental proposals at AGS[33] and at KEK.[34] In early 1987, the AGS (π^+, K^+) experiment was successfully performed. In the following, we will present the preliminary results of this

TABLE IV. Relevant Parameters for the (π^+, K^+) Measurements

Target	Thickness (gm/cm^2)	Run time (hrs)	π^+ intensity (1/sec)
^{9}Be	2.35	27	2×10^6
^{12}C	2 - 4	13.5	2×10^6, 1×10^7
^{13}C	2.0	23	1×10^7
^{16}O	3.0	434	2×10^6
^{28}Si	4.03	73.3	2×10^6
^{40}Ca	4.03	109.5	2×10^6, 1×10^7
^{51}V	2.89	23	1×10^7
^{89}Y	4.03	88	1×10^7

new (π^+, K^+) experiment.

The (π^+, K^+) experiment was performed at the Low Energy Separated Beam at AGS using the hypernuclear spectrometer "Moby-Dick." The beam momentum was chosen at 1050 MeV/c, which is near the peak of the $n(\pi^+, K^+)\Lambda$ elementary cross section. All measurements were made with the kaon spectrometer situated at $\theta_{lab} = 10°$. The (π^+, K^+) spectra were obtained on ^{9}Be, ^{12}C, ^{13}C, ^{16}O, ^{28}Si, ^{40}Ca, ^{51}V, and ^{89}Y. Relatively high intensity pion flux up to 10^7 per beam spill was used in this experiment. Table IV lists the pertinent information concerning measurements on various nuclear targets.

Figure 11(a) shows the $^{12}C(\pi^+, K^+)$ spectra measured in our experiment using an active scintillator target. The $[(p_{3/2})_n^{-1}(s_{1/2})_\Lambda]\ 1^-$ ground state and $[(p_{3/2})_n^{-1}(p_{3/2})_\Lambda]\ 2^+$ state of $^{12}_{\Lambda}C$ stand out clearly above the quasi-free background. Since a bound Λ-nuclear state eventually decays by releasing considerable amount of energy, one expects to discriminate the hypernuclear states from the quasi-free background by examining the energy deposit in the active target. Figure 11(b) shows that the quasi-free background is indeed significantly reduced when a large energy deposit in the target is required.

The (π^+, K^+) spectra obtained on the ^{28}Si and ^{89}Y targets are shown in Figs. 12-13. The remarkably low experimental background allowed us to observe transitions with cross sections as low as 0.1 μb/sr. Indeed we have good evidence that the $^{28}_{\Lambda}Si$ and $^{89}_{\Lambda}Y$ ground states are populated in the (π^+, K^+) reaction. In addition to the ground state,

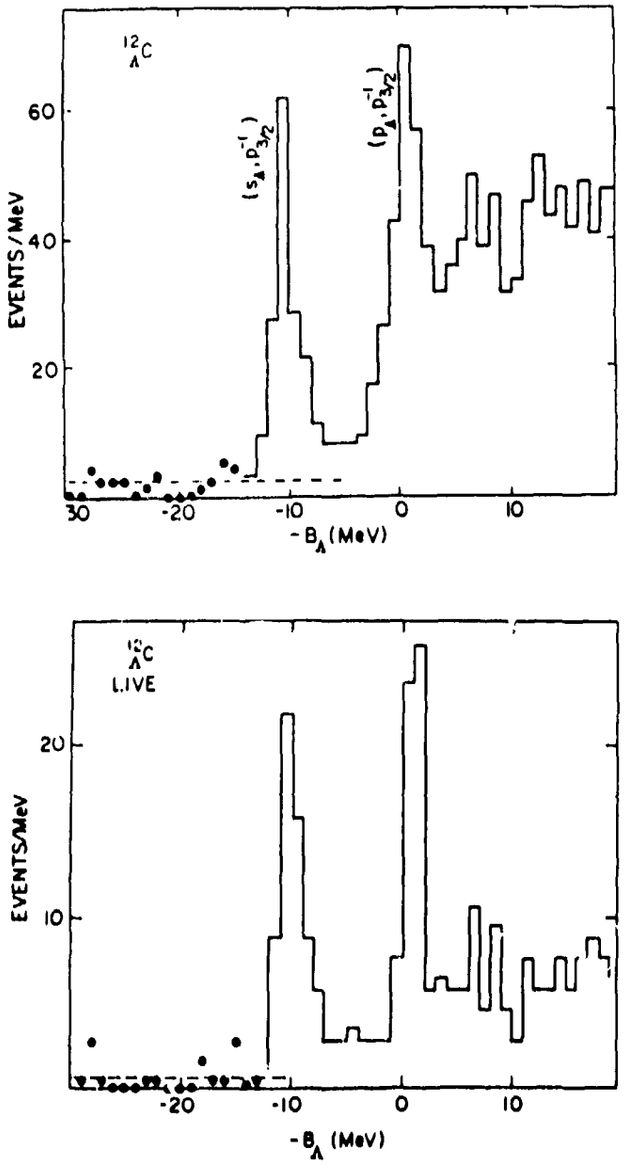

Fig. 11. $^{12}C(\pi^+, K^+)^{12}_{\Lambda}C$ spectra measured at 1050 MeV/c and $\theta_{lab} = 10°$. Quasifree background is suppressed in (b) which requires large energy deposited in the active target.

other peaks are observed in the spectra. These peaks are tentatively identified as various neutron-hole lambda-particle states. The tentative shell model configurations for these states are shown in Figs. 12–13. The large momentum transfer occurring in the (π^+, K^+) reaction makes it impossible to determine the spin of hypernuclear states excited in this reaction. Fortunately, it was shown[30,35] that the magnitude of the $^{12}C(\pi^+, K^+)^{12}_{\Lambda}C$ cross sections can be well described by DWIA calculations. It is therefore very important to

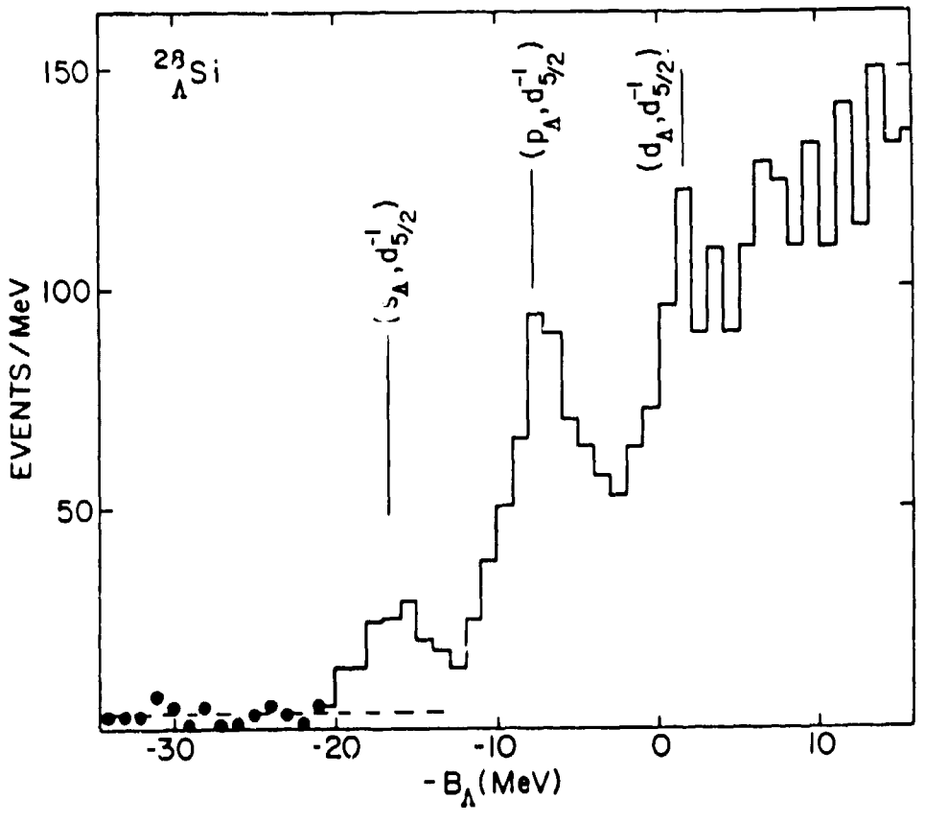

Fig. 12. $^{28}Si(\pi^+, K^+)^{28}_{\Lambda}Si$ spectrum measured at 1050 MeV/c and $\theta_{lab} = 10°$.

perform DWIA calculations for the nuclei studied in the present experiment. Preliminary results[36] give good agreement between the experiment and theory is obtained, supporting our assignments of the configurations of various peaks in Figs. 12–13.

In Fig. 14 we plot the binding energies of the ground states observed in the present (π^+, K^+) experiment as a function of $A^{-2/3}$, where A is the mass number of the target. Since the Λ-hypernuclear ground state corresponds to a Λ-particle occupying an $s_{1/2}$ orbital, the binding energy for a Λ-particle in a square-well potential with constant depth is proportional to $A^{-2/3}$. Figure 14 shows that this simple prescription describes the binding energy data very well. It is clear that one can use more realistic shape, such as Woods-Saxon, for the Λ-nucleus potential. Dover and Millener showed that a Woods-Saxon potential with a depth of 29.34 MeV can describe very well[37] the binding energies not only for the $s_{1/2}$ Λ-orbital but also for the p, d and f Λ-orbitals. The success of the shell model to describe the Λ binding energies in heavy nuclei tends to support the view that Λ particle maintains its identity deeply inside the nuclei. However, it is probably unreasonable to expect large effects caused by possible partial-deconfinement of Λ, and it is important to further improve the accuracy (such as the energy resolution) for a more

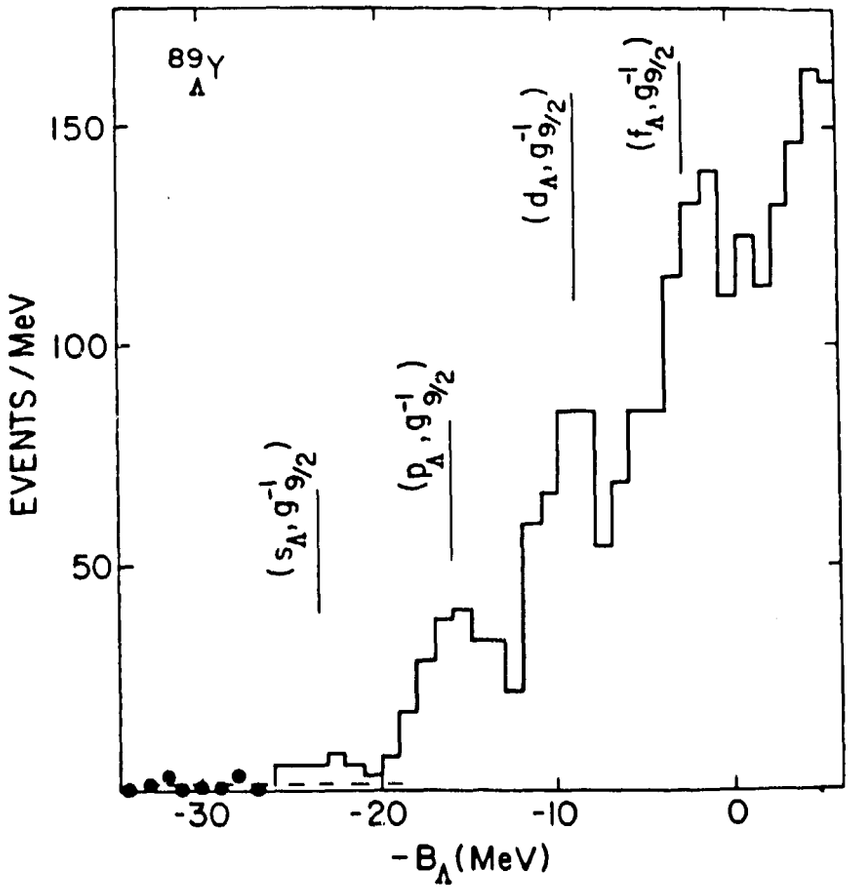

Fig. 13. $^{89}Y(\pi^+, K^+)^{89}_{\Lambda}Y$ spectrum measured at 1050 MeV/c and $\theta_{lab} = 10°$.

sensitive search of such effects. We refer to the paper by Dover[37] for a more detailed discussion on this subject.

In summary, the recent (π^+, K^+) results from AGS clearly demonstrated the usefulness of this reaction for investigating hypernuclear physics. It would be interesting in the future to measure the $p(\pi^+, K^+)$ reaction on even heavier nuclei such as ^{208}Pb. Furthermore, one can explore the feasibility of the $(\pi^+, K^+\gamma)$ coincidence experiment as a tool for high-resolution hypernuclear spectroscopy. Finally, the $(\pi^-, K^+)\Sigma^-$ elementary process could be considered as a means for producing Σ-hypernuclei. We conclude this paper by emphasizing that medium energy pion beams (0.5 GeV/c $< P_\pi <$ 2 GeV/c) offer great opportunity for future advances in medium energy nuclear physics.

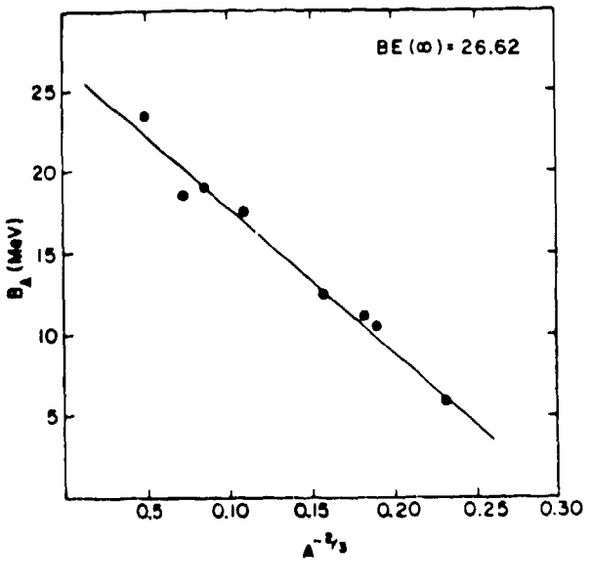

Fig. 14. Ground state binding energies observed in the (π^+, K^+) experiment plotted as a function of $A^{-2/3}$.

REFERENCES

1. Review of Particle Properties, Phys. Lett. 170B, 1 (1986).
2. V. Flaminio *et al.*, CERN-HERA 79-03 (1979).
3. O. Guisan *et al.*, Nucl. Phys. B32, 681 (1971).
4. V. V. Barmin *et al.*, Sov. J. Nucl. Phys. 28, 780 (1979).
5. V. D. Apokin *et al.*, Sov. J. Nucl. Phys. 35, 219 (1982).
6. V. V. Arkhipov *et al.*, Sov. J. Nucl. Phys. 39, 76 (1984).
7. LAMPF Proposals E852 and E934, Spokesmen: J. C. Peng and J. E. Simmons.
8. H. W. Baer *et al.*, Phys. Rev. Lett. 45, 982 (1980).
9. R. D. Baker *et al.*, Nucl. Phys. B156, 93 (1979).
10. H. Pilkuhn, The Interactions of Hadrons, North-Holland, Amsterdam (1967).
11. D. Dumbrajs *et al.*, Nucl. Phys. B216, 277 (1983).
12. S. F. Tuan, Phys. Rev. 139, B1393 (1965).
13. R. S. Bhalerao and L. C. Liu, Phys. Rev. Lett. 54, 865 (1985).
14. J. C. Peng, AIP Conference Proceedings No. 133, 255 (1985).

15. Q. Haider and L. C. Liu, Phys. Lett. 172, 257 (1986).

16. J. C. Peng *et al.*, Phys. Rev. Lett. 58, 2027 (1987).

17. D. A. Sparrow, Phys. Lett. 58B, 309 (1975).
R. H. Landau, Phys. Rev. C15, 2127 (1977).
W. J. Gerace *et al.*, Phys. Rev. C22, 1197 (1980).

18. J. Källne *et al.*, Phys. Rev. Lett. 42, 159 (1979).
M. D. Cooper *et al.*, Phys. Rev. C25, 438 (1982).

19. J. S. McCarthy, I. Sick, and R. R. Whitney, Phys. Rev. C15, 1396 (1977).

20. E. P. Colton *et al.*, Nu Instr. and Meth. 178, 95 (1980).

21. H. Brody *et al.*, Phys. Rev. D9, 1917 (1974).

22. H. W. Baer *et al.*, Nucl. Instr. and Meth. 180, 445 (1981).

23. Li Yang-guo and Chiang Huan-Ching, Nucl. Phys. A454, 720 (1986).

24. L. C. Liu, private communication, 1987.

25. K. S. Kolbig and B. Margolis, Nucl. Phys. B6, 85 (1968).

26. L. O. Abrahamian *et al.*, Phys. Lett. 44B, 301 (1973).

27. B. Povh, Ann. Rev. Nucl. Part. Sci. 28, 1 (1978).

28. C. B. Dover, L. Ludeking, and G. E. Walker, Phys. Rev. C22, 2073 (1980).

29. AGS proposal 758, Spokesman: H. A. Thiessen.

30. C. Milner *et al.*, Phys. Rev. Lett. 54, 1237 (1985).

31. T. Cantwell *et al.*, Nucl. Phys. A232, 445 (1974).

32. E. V. Hungerford and L. C. Biedenharn, Phys. Lett. 142B, 232 (1984).

33. AGS Proposal 798, Spokesmen: J. C. Peng and P. Pile.

34. KEK proposal, Spokesmen: O. Hashimoto and T. Shibata.

35. J. C. Peng, Nucl. Phys. A450, 129C (1986).

36. J. Millener, private communication, 1987.

37. C. B. Dover, Proceedings of the International Symposium on Medium Energy Physics, Beijing, China (1987).